Quantum criticality in a metallic spin liquid

Y. Tokiwa[1*], J. J. Ishikawa[2], S. Nakatsuji[2,3] and P. Gegenwart[1†]

When magnetic order is suppressed by frustrated interactions, spins form a highly correlated fluctuating 'spin liquid' state down to low temperatures. The magnetic order of local moments can also be suppressed when they are fully screened by conduction electrons through the Kondo effect. Thus, the combination of strong geometrical frustration and Kondo screening may lead to novel types of quantum phase transition. We report low-temperature thermodynamic measurements on the frustrated Kondo lattice $Pr_2Ir_2O_7$, which exhibits a chiral spin liquid state below 1.5 K as a result of the frustrated interaction between Ising 4*f* local moments and their interplay with Ir conduction electrons. Our results provide a first clear example of zero-field quantum critical scaling that emerges in a spin liquid state of a highly frustrated metal.

Strong quantum fluctuations pertinent to geometrically frustrated quantum spin systems could suppress long-range order and induce spin liquid ground states. It has been proposed that Kondo lattice systems undergo a quantum phase transition from long-range ordered to metallic spin liquid states as quantum fluctuations grow stronger[1–3]. In Fig. 1, the relation between spin liquid and quantum critical states is illustrated. Here the parameter Q is a measure of the strength of quantum fluctuations, induced by competing interactions or geometrical frustration. For insulators it could be quantified by the frustration parameter $f = |\theta| / T_{MO}$, which measures the ratio of the absolute value of the Weiss temperature to the ordering temperature. Insulators with sufficiently large frustration of their local magnetic moments form a strongly correlated fluctuating state, a so-called spin liquid, at temperatures below $|\theta|$. For the fully frustrated case the ordering temperature is completely suppressed, giving rise to a quantum critical point (QCP), and the spin liquid phase extends down to zero temperature. On the other hand, Kondo screening in metals acts in reducing the size of local magnetic moments and suppresses magnetic order as well. As a result, in the presence of Kondo interactions, already a moderately strong frustration can induce quantum criticality by suppression of magnetic order to zero temperature. A line of quantum critical points emerges (see red line in Fig. 1) which at $T = 0$ connects the insulating spin liquid with the metallic sector of the phase diagram. Different types of paramagnetic state are currently discussed for *f*-electron based heavy-fermion metals. For sufficiently large Kondo coupling, K, the f-moments are bound in Kondo singlets. The resulting Fermi liquid (FL) has a 'large' Fermi surface volume including the f electrons. However, the possibility of an f-selective Mott transition due to a breakdown of Kondo screening has been extensively discussed in recent years[4–6]. It is expected that, for sufficiently strong Q, a novel paramagnetic phase P_S forms, with a 'small' Fermi volume determined by conduction electrons only[3,7,8]. As the moments in this state are neither Kondo screened nor magnetically ordered, they are expected to form a spin liquid. Experimentally, this phase is largely unexplored and its relation to the proposed line of QCPs connecting to the insulating spin liquid is unknown.

We focus on the pyrochlore iridate $Pr_2Ir_2O_7$, with local Pr^{3+} magnetic moments and a small concentration of Ir 5d conduction electrons giving rise to a weak Kondo coupling[9]. Crystal electric field (CEF) splitting leads to a magnetic non-Kramers doublet ground state and the lowest CEF excited state at 162 K (ref. 9). Those moments are located on the edges of corner-sharing tetrahedra, leading to a geometrically frustrated magnetic interaction. The effect of strong geometrical frustration is evidenced by the absence of magnetic ordering on cooling the system to very low temperatures, despite a Curie–Weiss temperature $\Theta = -20$ K, determined from the temperature dependence of the susceptibility above 100 K (ref. 9) and the estimated nearest-neighbour ferromagnetic interaction of 1.4 K (ref. 10). The metamagnetic transition observed only along the [111] axis confirms the spin ice formation while the transition field of 2.3 T yields a ferromagnetic interaction scale of 1.4 K. The combination of a finite Kondo coupling K and the strong geometrical frustration places $Pr_2Ir_2O_7$ in the P_S phase of Fig. 1. An intriguing observation in this system is the spontaneous Hall conductivity below 1.5 K in the absence of magnetic order[10]. This was attributed to the formation of a chiral spin liquid. Here, the non-zero spin chirality acts as a fictitious field and breaks time reversal symmetry. This is distinct from the topological Hall signal due to skyrmions and its related non-Fermi liquid phase in MnSi (ref. 11).

The manifold of degenerate configurations of spin ice systems results in the Pauling entropy $(R/2)\ln(3/2)$ (ref. 12). Classical spin ice systems, such as $Dy_2Ti_2O_7$ (ref. 12) and $Ho_2Ti_2O_7$ (ref. 13) develop two-in two-out configurations from a completely uncorrelated state at high temperatures. Their specific heat, $C(T)$, exhibits a characteristic maximum on cooling, releasing the entropy of $R[\ln(2) - (1/2)\ln(3/2)]$. Qualitatively similar behaviour has also been found for insulating $Pr_2Zr_2O_7$ (ref. 14). The ground state of spin ice is controversially discussed[15]. $Pr_2Ir_2O_7$ satisfies the requirements of spin ice formation, namely Ising type 4*f* magnetic moments and ferromagnetic nearest-neighbour interactions. However, the presence of conduction electrons gives rise to an RKKY-type interaction which has been proposed to mediate spin chirality[16] or spiral dipolar and XY-quadrupolar ordering[17].

[1]I. Physikalisches Institut, Georg-August-Universität Göttingen, 37077 Göttingen, Germany, [2]Institute for Solid State Physics, University of Tokyo, Kashiwa 277-8581, Japan, [3]PRESTO, Japan Science and Technology Agency (JST), 4-1-8 Honcho Kawaguchi, Saitama 332-0012, Japan.
†Present address: Experimental Physics VI, Center for Electronic Correlations and Magnetism, University of Augsburg, 86159 Augsburg, Germany.
*e-mail: ytokiwa@gmail.com

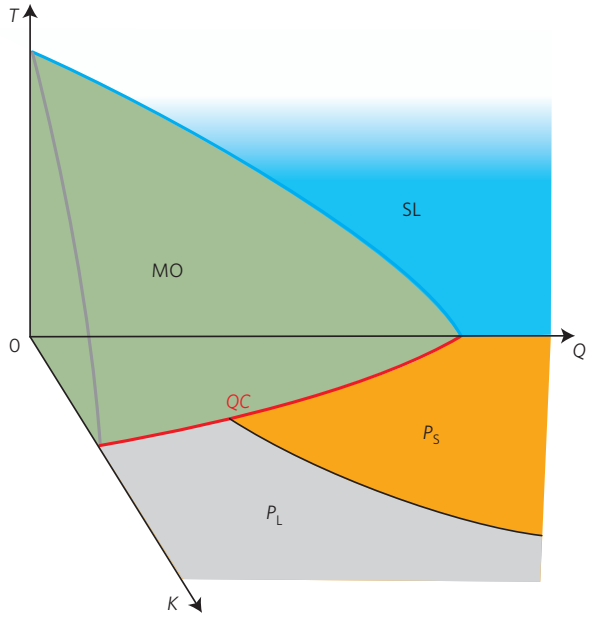

Figure 1 | Schematic phase diagram for geometrically frustrated Kondo lattice systems. Different phases are shown as a function of temperature (T), strength of quantum fluctuations (Q) and Kondo coupling (K). The blue phase in the sector without Kondo coupling indicates an insulating spin liquid (SL). A line of quantum critical points (in red) bounds the long-range magnetic order (MO; green region) at $T=0$. The black line in the $T=0$ plane indicates the transition between paramagnetic states with large (P_L) and small (P_S) Fermi surfaces, whose continuation within the MO state has been omitted for clarity[3,8]. The proposed and yet unexplored P_S phase comprises unscreened local moments in a metallic spin liquid state[2,7].

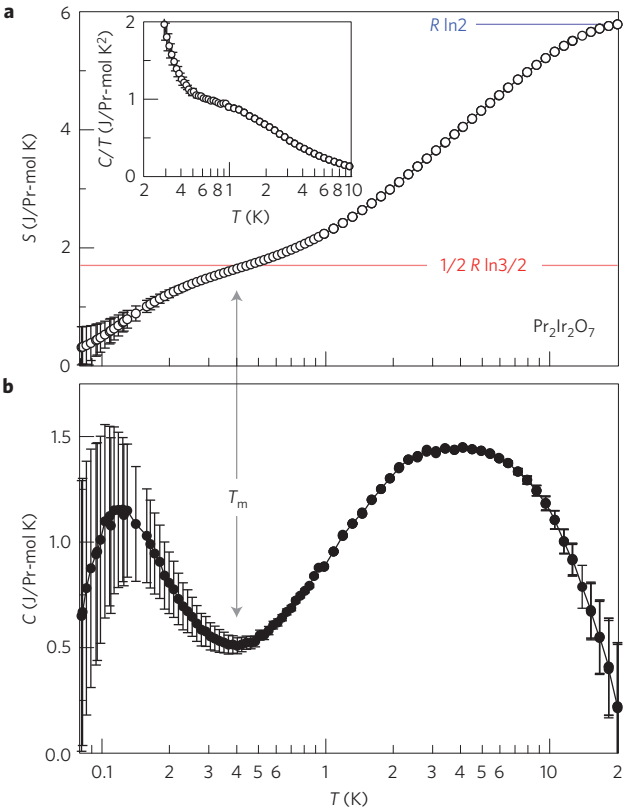

Figure 2 | Low-temperature specific heat and entropy of $Pr_2Ir_2O_7$. **a**, Magnetic entropy from the CEF ground state doublet calculated from the specific heat data under the assumption that the entropy at 20 K approaches the expected value $R\ln(2)$. Entropy for the crystalline electric field doublet, $R\ln(2)$, and Pauling entropy, $(R/2)\ln(3/2)$, are marked by blue and red lines, respectively. The inset shows the specific heat divided by temperature, C/T, on a logarithmic temperature scale. **b**, Specific heat C as a function of temperature. Phonon contribution, the contribution due to the excited crystalline electric field states, as well as the nuclear contribution have been subtracted (Supplementary Information). The large error bars at low temperatures are caused by the uncertainty of the subtraction of the nuclear contribution. The onset of the low-temperature upturn in $C(T)$, indicative of the quantum melting of spin ice at $T_m=0.4$ K, is marked by the arrows.

We have studied the thermodynamic properties of $Pr_2Ir_2O_7$ down to below 100 mK.

Figure 2 shows our specific heat and entropy data on single-crystalline $Pr_2Ir_2O_7$. On cooling, the specific heat passes the characteristic spin ice maximum and decreases until it reaches a minimum at 0.4 K. At this temperature the entropy approaches the Pauling value, indicating that the formation of two-in two-out spin ice configurations is completed in all of the tetrahedra. Further cooling below 0.4 K yields a huge enhancement of the specific heat divided by temperature (see Fig. 2 inset). In the absence of a clear phase transition anomaly we associate the corresponding entropy reduction to the melting of spin ice configurations by quantum fluctuations at $T_m \approx 0.4$ K (arrow in Fig. 2; ref. 18).

Next, we turn our attention to the detection of quantum criticality in this material. The magnetic Grüneisen ratio $\Gamma_H = 1/T(dT/dH)_S$, which measures the change of temperature with magnetic field under adiabatic conditions, generically diverges in the approach of any QCP (ref. 19). This results from the entropy accumulation in the quantum critical regime and has been experimentally confirmed, for example, at the field-tuned QCP in the heavy-fermion metal $YbRh_2Si_2$ (ref. 20). Assuming that critical behaviour is governed by a single diverging timescale near the QCP, universal scaling of physical properties such as thermal expansion, specific heat or magnetization as a function of $T/(H-H_c)^{\nu z}$, where ν is the correlation length exponent and z is the dynamical exponent, is expected[19]. Such scaling results from the competition of quantum and thermal fluctuations near the QCP. The distance to the QCP, $H-H_c$, which is related to quantum fluctuations, influences the critical scaling, in contrast to the classical critical scaling, where the critical components of physical quantities depend only on the reduced temperature, $|T-T_c|/T_c$ (where T_c is the critical temperature). Observation of $T/(H-H_c)^{\nu z}$ scaling over a substantial parameter range therefore acts as proof of quantum critical behaviour and determines the exact position of the QCP, that is, the value of the critical magnetic field H_c. In $Sr_3Ru_2O_7$ (ref. 21), $CeCu_{5.9}Au_{0.1}$ (ref. 22) and $YbRh_2Si_2$ (ref. 23), several physical quantities were shown to exhibit quantum critical scaling in a wide range in the H–T phase space around their QCPs.

The magnetic Grüneisen ratio can also be expressed by the magnetization M and specific heat C, as $\Gamma_H = -(dM/dT)/C$ (ref. 19). Because for $Pr_2Ir_2O_7$ the low-temperature magnetization is almost isotropic at fields below approximately 0.5 T (ref. 10), we do not expect that the zero-field quantum critical behaviour of the magnetic Grüneisen ratio discussed in the following exhibits an anisotropy with respect to the field orientation at low fields. Figure 3 shows Γ_H/H of $Pr_2Ir_2O_7$ at various magnetic fields applied parallel to the [111] direction, whereas data for the field along [100] are shown in Supplementary Fig. 2. On cooling, the magnetic Grüneisen ratio at low field diverges according to $T^{-3/2}$ over almost one decade in temperature down to about 0.4 K, providing evidence for quantum critical behaviour[19]. Remarkably, this temperature coincides with the reduction of the entropy below the Pauling value (T_m in Fig. 2). Whatever causes the 'melting' of the spin

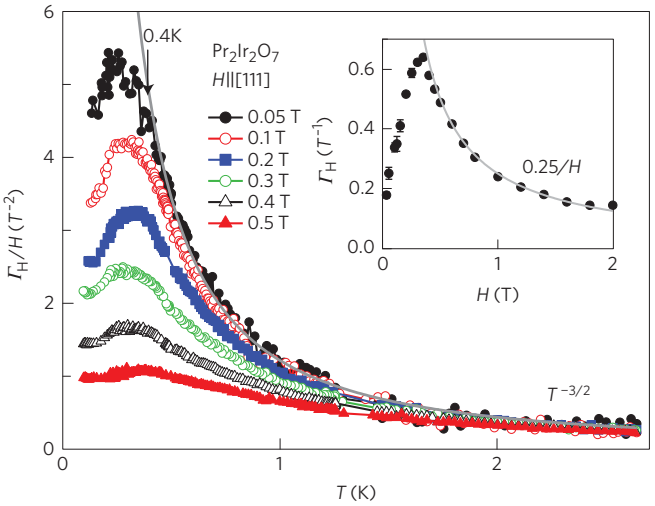

Figure 3 | Divergent behaviour of the magnetic Grüneisen ratio, Γ_H, of $Pr_2Ir_2O_7$ as function of temperature. Γ_H is measured at magnetic fields applied parallel to the [111] direction. The divergence with a power law $\sim T^{-3/2}$ is indicated by the grey solid line. Arrow at 0.4 K indicates the temperature below which Γ_H deviates from the power-law divergence. Inset shows the field dependence of the constant Γ_H values in the low-temperature quantum paramagnetic regime at $T \to 0$. Grey solid line indicates $0.25/H$.

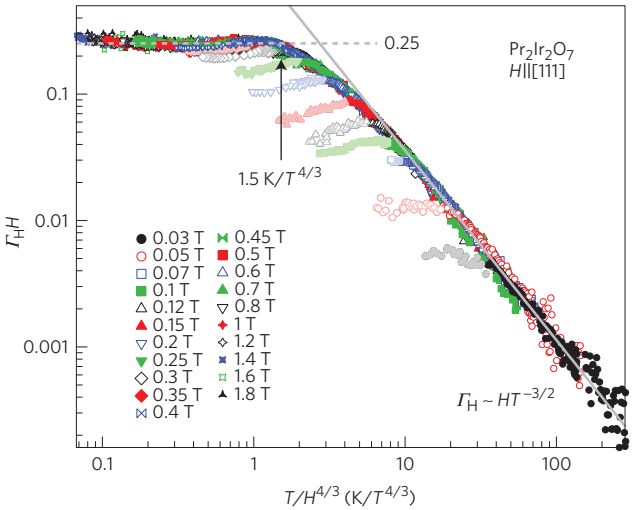

Figure 4 | Evidence of a zero-field quantum critical point in $Pr_2Ir_2O_7$. Quantum critical scaling of the magnetic Grüneisen ratio, Γ_H, is shown by plotting $\Gamma_H H$ versus $T/H^{4/3}$. The magnetic field is applied parallel to the [111] direction. Data points from the phase space regime, indicated by a blue dotted line in Fig. 5, that deviate from the scaling behaviour are plotted in pastel colours. Constant $\Gamma_H H = 0.25$ in the quantum paramagnetic state is indicated by a grey dotted line. The arrow at 1.5 $T/H^{4/3}$ indicates the crossover temperature between the quantum paramagnetic and quantum critical behaviour. Solid grey line indicates the $HT^{-3/2}$ dependence of Γ_H within the quantum critical state.

ice state, it also suppresses quantum criticality. As the magnetic field is increased, Γ_H/H becomes independent of temperature at lowest temperatures, indicating the formation of a quantum paramagnetic state; that is, a non-critical quantum spin liquid. Assuming universal scaling near a QCP (ref. 19), it is theoretically expected that $\Gamma_H = -G_r/(H - H_c)$ in the quantum paramagnetic state. The universal prefactor $G_r = \nu(d - y_0 z)/y_0$ is determined by the dimensionality d and the exponent y_0 of the temperature dependence of the specific heat ($C \sim T^{y_0}$). For $Pr_2Ir_2O_7$ the large uncertainty in the subtraction of the nuclear specific heat makes it impossible to reliably determine y_0. The constant Γ_H values obtained at lowest temperatures follow the expected $(H - H_c)^{-1}$ dependence and are remarkably well fitted by $H_c = 0 \pm 0.04$ T, suggesting a zero-field QCP (Fig. 3 inset). As explained in the Supplementary Information, slightly different scaling relations are expected in such a case, because of the quadratic coupling of H with order parameter. As a result, the Grüneisen ratio $\Gamma_H H = f(T/H^{2\nu z})$, where f is a universal scaling function. Furthermore, for $T \to 0$, the magnetic Grüneisen ratio diverges toward zero field as $\Gamma_H = -2G_r/H$ in the case $H_c = 0$. Experimentally, we found $2G_r = -0.25 \pm 0.03$ for $H \parallel [111]$. A slight deviation from the $\Gamma_H = -2G_r/H$ scaling is found above 2 T, on approaching the transition to the 3-in 1-out state at 2.3 T (ref. 10), which breaks the ice-rule. Thus, quantum criticality is related to the degeneracy within the spin ice state.

We further examine quantum criticality in $Pr_2Ir_2O_7$ by rescaling the Γ_H data. In Fig. 4 the magnetic Grüneisen ratio data are shown as $\Gamma_H H$ versus $T/H^{4/3}$. The measured data collapse on a common curve for about four decades in the x-axis and more than three decades in the y-axis. This confirms that the system is located at a zero-field QCP. The scaling plot clearly shows the crossover between the quantum critical and quantum paramagnetic states, which are characterized by $\Gamma_H \sim HT^{-3/2}$ and $\Gamma_H = 0.25/H$ (temperature independent), respectively (also see inset of Fig. 3). There is a certain regime in temperature–field phase space for which scaling does not hold. At low fields, this includes temperatures below 0.4 K and extends up to about 0.35 T, whereas at larger fields all data follow scaling down to lowest temperatures. The same scaling behaviour of $\Gamma_H H$ versus $HT^{-3/2}$ is found also for $H \parallel [100]$ (Supplementary Fig. 3). However, the value of $2G_r = -0.37 \pm 0.03$ in the quantum paramagnetic state at low temperatures is different from -0.25 for $H \parallel [111]$. As the field direction of [111] is known as a special direction, stabilizing the kagome-ice state[24], the anisotropy of G_r may be a result of quantum paramagnetic states with different y_0 along the two field directions. Generically, as found, for example, for the QCP in $CeCoIn_5$ (ref. 25), G_r is isotropic (see discussion in the Supplementary Information).

Figure 5 shows the T–H phase diagram, where the colour coding indicates the size of the magnetic Grüneisen ratio, which exhibits quantum critical scaling for temperatures below 3 K and fields below 2 T. Only very close to the zero-field QCP this scaling is violated in a regime, which is bound by the blue dotted line. In the absence of a clear phase transition the nature of this state is unknown.

The experimentally observed scaling exponents allow one to characterize quantum criticality in $Pr_2Ir_2O_7$. If quantum criticality is governed by a single diverging timescale[19], the magnetic Grüneisen ratio scales like $T/(H)^{2\nu z}$, yielding νz=2/3. This differs from the expectation within the itinerant Hertz–Millis–Moriya theory for magnetic QCPs. The latter predicts νz=1 for antiferromagnetism and νz=3/2 for ferromagnetism[19]. As our system has a local moment character and only a very weak Kondo interaction, it is not surprising that the observed exponents differ from the itinerant model for spin-density-wave instabilities. Furthermore, within the quantum paramagnetic state we observe $\Gamma_H H = 0.25$ and 0.37, implying $-\nu(d - y_0 z)/y_0 = 0.125$ and 0.185 for $H \parallel [111]$ and [100], respectively. These relations will place strong constraints on theoretical modelling of quantum criticality in $Pr_2Ir_2O_7$ (ref. 26).

The previous observation of a spontaneous Hall effect, despite the absence of dipolar magnetic order, suggests a chiral spin liquid state in the temperature range[10] where our study reveals zero-field quantum criticality. Taken together, these observations support a novel type of 'quantum critical spin liquid' state that may be expected from the global phase diagram of Kondo lattice materials. The observed quantum critical scaling is different from what has

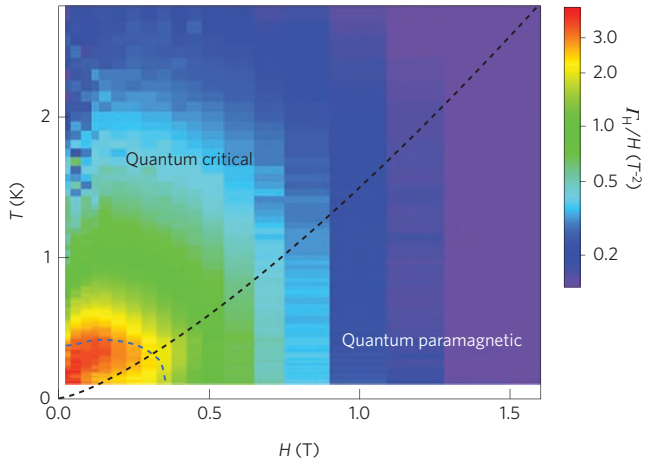

Figure 5 | Colour-coded contour plot of the Grüneisen ratio divided by magnetic field, Γ_H/H, of $Pr_2Ir_2O_7$ in H–T phase space. Note the logarithmic scale for the colour-coding. The crossover temperature between the quantum critical and quantum paramagnetic regimes follows a $H^{4/3}$ dependence and is indicated by the black dotted line. The blue dotted lines enclose the phase space for which the magnetic Grüneisen ratio deviates from the scaling behaviour (data points in pastel colour in Fig. 4).

been predicted for itinerant systems with a large Fermi volume, suggesting our system be placed within the 'P_S' sector in the phase diagram. Several novel quantum phases such as unconventional superconductivity[27] or electronic nematic ordering[28] have been found in clean metals near quantum critical points. In this respect the state below 0.4 K in $Pr_2Ir_2O_7$ requires further attention.

Methods

Single crystals of $Pr_2I_2O_7$ were grown by the flux method, described in detail in ref. 29. The magnetic Grüneisen ratio $\Gamma_H = 1/T(dT/dH)_S$ was obtained by measuring the magnetocaloric effect $(dT/dH)_S$ by means of the alternating field technique[30] in a dilution refrigerator equipped with a superconducting magnet. Specific heat was measured by the quasi-adiabatic heat pulse method in a dilution refrigerator. The equilibration time window was fixed to 5 s above 0.4 K and was varied continuously from 5 to 40 s from 0.4 to 0.1 K, as the heat flow within the sample becomes slow owing to the large nuclear specific heat. Specific heat measurements in the high-temperature region above 2 K were performed using a commercial Quantum Design Physical Property Measurement System.

References

1. Si, Q. Global magnetic phase diagram and local quantum criticality in heavy fermion metals. *Physica B* **378–380,** 23–27 (2006).
2. Vojta, M. From itinerant to local-moment antiferromagnetism in Kondo lattices: Adiabatic continuity versus quantum phase transitions. *Phys. Rev. B* **78,** 125109 (2008).
3. Custers, J. *et al.* Evidence for a non-Fermi-liquid phase in Ge-substituted $YbRh_2Si_2$. *Phys. Rev. Lett.* **104,** 186402 (2010).
4. Coleman, P., Pepin, C., Si, Q. & Ramazashvili, R. How do Fermi liquids get heavy and die? *J. Phys. Condens. Matter* **13,** R723–R738 (2001).
5. Si, Q., Rabello, S., Ingersent, K. & Smith, J. L. Locally critical quantum phase transitions in strongly correlated metals. *Nature* **413,** 804–808 (2001).
6. Paschen, S. *et al.* Hall-effect evolution across a heavy-fermion quantum critical point. *Nature* **432,** 881–885 (2004).
7. Senthil, T., Sachdev, S. & Vojta, M. Fractionalized Fermi liquids. *Phys. Rev. Lett.* **90,** 216403 (2003).
8. Si, Q. & Paschen, S. Quantum phase transitions in heavy fermion metals and Kondo insulators. *Phys. Status Solidi B* **250,** 425–438 (2013).
9. Nakatsuji, S. *et al.* Metallic spin-liquid behaviour of the geometrically frustrated Kondo lattice $Pr_2Ir_2O_7$. *Phys. Rev. Lett.* **96,** 087204 (2006).
10. Machida, Y., Nakatsuji, S., Onoda, S., Tayama, T. & Sakakibara, T. Time-reversal symmetry breaking and spontaneous Hall effect without magnetic dipole order. *Nature* **463,** 210–213 (2010).
11. Ritz, R. *et al.* Formation of a topological non-Fermi liquid in MnSi. *Nature* **497,** 231–234 (2013).
12. Ramirez, A. P., Hayashi, A., Cava, R. J., Siddharthan, R. & Shastry, B. S. Zero-point entropy in 'spin ice'. *Nature* **399,** 333–335 (1999).
13. Bramwell, S. T. *et al.* Spin correlations in $Ho_2Ti_2O_7$: A dipolar spin ice system. *Phys. Rev. Lett.* **87,** 047205 (2001).
14. Kimura, K. *et al.* Quantum fluctuations in spin-ice-like $Pr_2Zn_2O_7$. *Nature Commun.* **4,** 1934 (2013).
15. Pomaranski, D. *et al.* Absence of Pauling's residual entropy in thermally equilibrated $Dy_2Ti_2O_7$. *Nature Phys.* **9,** 353–356 (2013).
16. Flint, R. & Senthil, T. Chiral RKKY interaction in $Pr_2Ir_2O_7$. *Phys. Rev. B* **87,** 125147 (2013).
17. Lee, S., Paramekanti, A. & Kim, Y. B. RKKY interactions and the anomalous Hall effect in metallic rare-earth pyrochlores. *Phys. Rev. Lett.* **111,** 196601 (2013).
18. Onoda, S. & Tanaka, Y. Quantum melting of spin ice: emergent cooperative quadrupole and chirality. *Phys. Rev. Lett.* **105,** 047201 (2010).
19. Zhu, L., Garst, M., Rosch, A. & Si, Q. Universally diverging Grüneisen parameter and the magnetocaloric effect close to quantum critical points. *Phys. Rev. Lett.* **91,** 066404 (2003).
20. Tokiwa, Y., Radu, T., Geibel, C., Steglich, F. & Gegenwart, P. Divergence of the magnetic Grüneisen ratio at the field-induced quantum critical point in $YbRh_2Si_2$. *Phys. Rev. Lett.* **102,** 066401 (2009).
21. Gegenwart, P., Weickert, F., Garst, M., Perry, R. S. & Maeno, Y. Metamagnetic quantum criticality in $Sr_3Ru_2O_7$ studied by thermal expansion. *Phys. Rev. Lett.* **96,** 136402 (2006).
22. Schroeder, A. *et al.* Onset of antiferromagnetism in heavy-fermion metals. *Nature* **407,** 351– 355 (2000).
23. Custers, J. *et al.* The break-up of heavy electrons at a quantum critical point. *Nature* **424,** 524– 527 (2003).
24. Hiroi, Z., Matsuhira, K., Takagi, S., Tayama, T. & Sakakibara, T. Specific heat of kagomé ice in the pyrochlore oxide $Dy_2Ti_2O_7$. *J. Phys. Soc. Jpn* **72,** 411–418 (2003).
25. Tokiwa, Y., Bauer, E. D. & Gegenwart, P. Zero-field quantum critical point in $CeCoIn_5$. *Phys. Rev. Lett.* **111,** 107003 (2013).
26. Moon, E-G., Cenke, X., Kim, Y. B. & Balents, L. Non-Fermi-liquid and topological states with strong spin–orbit coupling. *Phys. Rev. Lett.* **111,** 206401 (2013).
27. Mathur, N. D. *et al.* Magnetically mediated superconductivity in heavy fermion compounds. *Nature* **394,** 39–43 (1998).
28. Borzi, R. A. *et al.* Formation of a nematic fluid at high fields in $Sr_3Ru_2O_7$. *Science* **315,** 214–217 (2007).
29. Millican, J. N. *et al.* Crystal growth and structure of $R_2Ir_2O_7$ (R = Pr, Eu) using molten KF. *Mater. Res. Bull.* **42,** 928–934 (2007).
30. Tokiwa, Y. & Gegenwart, P. High-resolution alternating-field technique to determine the magnetocaloric effect of metals down to very low temperatures. *Rev. Sci. Instrum.* **82,** 013905 (2011).

Acknowledgements

The authors acknowledge discussions with L. Balents, M. Brando, J.G. Donath, M. Garst, Yong-Baek Kim, K. Kimura, Q. Si, C. Stingl, M. Vojta and K. Winzer. This work has been supported by the German Science Foundation through FOR 960 (Quantum phase transitions), the Helmholtz Virtual Institute VH521, and by Grants-in-Aid for Scientific Research (No. 25707030) from JSPS, and by PRESTO of JST. The use of the Materials Design and Characterization Laboratory at ISSP is gratefully acknowledged. This work was supported also in part by the National Science Foundation under Grant No. PHYS-1066293 and the hospitality of the Aspen Center for Physics.

Author contributions

Y.T., S.N. and P.G. planned the project. Measurements and analysis of the specific heat and magnetocaloric effect were performed by Y.T. The samples were synthesized and characterized by J.J.I. and S.N. Y.T., S.N. and P.G. discussed the results and prepared the manuscript.

Additional information

Supplementary information is available in the online version of the paper. Reprints and permissions information is available online at www.nature.com/reprints. Correspondence and requests for materials should be addressed to Y.T.

Competing financial interests

The authors declare no competing financial interests.